Energy-Conversion Properties of Vapor-Liquid-Solid–Grown Silicon Wire-Array Photocathodes

Shannon W. Boettcher *et al.*

Science **327**, 185 (2010);
DOI: 10.1126/science.1180783

Science (print ISSN 0036-8075; online ISSN 1095-9203) is published weekly, except the last week in December, by the American Association for the Advancement of Science, 1200 New York Avenue NW, Washington, DC 20005.

Energy-Conversion Properties of Vapor-Liquid-Solid–Grown Silicon Wire-Array Photocathodes

Shannon W. Boettcher, Joshua M. Spurgeon, Morgan C. Putnam, Emily L. Warren, Daniel B. Turner-Evans, Michael D. Kelzenberg, James R. Maiolo, Harry A. Atwater,* Nathan S. Lewis*

Silicon wire arrays, though attractive materials for use in photovoltaics and as photocathodes for hydrogen generation, have to date exhibited poor performance. Using a copper-catalyzed, vapor-liquid-solid–growth process, $SiCl_4$ and BCl_3 were used to grow ordered arrays of crystalline p-type silicon (p-Si) microwires on p^+-Si(111) substrates. When these wire arrays were used as photocathodes in contact with an aqueous methyl viologen$^{2+/+}$ electrolyte, energy-conversion efficiencies of up to 3% were observed for monochromatic 808-nanometer light at fluxes comparable to solar illumination, despite an external quantum yield at short circuit of only 0.2. Internal quantum yields were at least 0.7, demonstrating that the measured photocurrents were limited by light absorption in the wire arrays, which filled only 4% of the incident optical plane in our test devices. The inherent performance of these wires thus conceptually allows the development of efficient photovoltaic and photoelectrochemical energy-conversion devices based on a radial junction platform.

Highly purified planar crystalline Si provides the basis for high-efficiency photovoltaics and has shown promise as a photocathode material for the production of H_2 from water and sunlight (*1*). In this planar geometry, efficient devices require the use of high-purity Si to obtain minority-carrier diffusion lengths that are comparable to the long optical absorption depth (~200 μm) associated with the indirect band gap of Si (*2*). Semiconductor wire arrays are an attractive alternative to this planar geometry because they can possess both long optical paths for efficient light absorption and short transport distances so as to ensure collection of the photogenerated charge carriers before they recombine (*2*–*13*). A wire-array geometry should thus allow for the use of semiconductors in which the collection length of photogenerated minority carriers is much shorter than the optical penetration depth. Indeed, device-physics modeling has predicted that wire-array structures using Si with a minority-carrier diffusion length of less than 10 μm can achieve solar energy–conversion efficiencies of greater than 15% (*2*).

To date, device efficiencies for radial-junction Si photovoltaics and photoelectrodes fabricated by use of potentially inexpensive techniques, such as vapor-liquid-solid (VLS)–growth processes (*14*), have been low. The highest reported efficiencies are for single-nanowire devices in which the performance was normalized to the active portion of the single wire, that is, excluding contacts and empty area (*8*, *9*). Up to 3.4% efficiency under solar simulation has been observed for a p-type/intrinsic/n-type (p-i-n) Si nanowire, with a low open-circuit voltage of 260 mV (*7*). Macroscopic VLS-grown Si wire-array devices have exhibited poor efficiencies (~0.1%) in both liquid-junction (*3*, *4*) and solid-state (*10*, *11*) configurations. A key question is whether higher performance, in accord with theoretical predictions, can be obtained with wire-array energy-conversion devices through improved control over the bulk impurities, surface defects, and doping.

To evaluate this possibility, we grew p-type Si wire arrays from $SiCl_4$ [10 standard cubic centimeters per minute (sccm)], H_2 (500 sccm), and dilute BCl_3 at 1000°C at atmospheric pressure for 20 to 30 min on p^+-Si(111) substrates. These substrates had been photolithographically patterned with 3-μm-diameter by 300-nm-thick Cu VLS-growth catalyst islands that were confined within a 300-nm-thick thermal Si oxide (*15*, *16*). The resulting wires were ~100 μm long, ~1.6 μm in diameter, and arranged on a square lattice with a 7-μm pitch, resulting in a packing fraction of ~4% (Fig. 1, A and B). The resistivity of the wires, as measured with single-wire four-point-probe methods (*9*), was varied by changing the BCl_3 flow rate. Wires grown from 0.25% BCl_3 in H_2 at a flow rate of 1 sccm had a resistivity of 0.05 ± 0.01 ohm cm, corresponding to a majority-carrier concentration near 7×10^{17} cm^{-3}, and exhibited optimal photoelectrochemical properties relative to wires with other doping levels. Before photoelectrochemical evaluation, the samples were etched with aqueous solutions of $FeCl_3$, KOH, and HF, so as to remove the Cu catalyst, the outer ~50 nm of Si (including Cu contained at or near the surface), and the native oxide, respectively, without substantial etching of the patterned thermal oxide that surrounded the bases of the wires (Fig. 1, C and D).

Kavli Nanoscience Institute and Beckman Institute, 1200 East California Boulevard, California Institute of Technology, Pasadena, CA 91125, USA.

*To whom correspondence should be addressed. E-mail: nslewis@caltech.edu (N.S.L.); haa@caltech.edu (H.A.A.)

The energy-conversion properties of the p-type silicon (p-Si) wire arrays were evaluated in an aqueous electrolyte containing the redox couple methyl viologen ($MV^{2+/+}$), whose conformal liquid contact allowed for testing without introducing difficulties associated with the production of rectifying, conformal solid-state junctions, transparent conductors, or metallic grid contacts. This redox system produces a high barrier height on p-Si (*3*, *17*) and enables the straightforward evaluation of any differences in the junction behavior between planar p-Si samples and p-Si wire-array electrodes. The comparison was performed in a three-electrode cell configuration in order to directly evaluate the performance of the photocathodes, to minimize resistive losses, and to allow quantification of the concentration and kinetic overpotentials that would be variables in two-electrode photoelectrochemical devices (Fig. 2). Monochromatic 808-nm light was used to minimize the optical absorption of the reduced form of the $MV^{2+/+}$ couple (*18*). This wavelength of light also has a relatively long optical-penetration depth of 11 μm in Si, which stresses the ability to collect photogenerated charge carriers produced deeply in the absorbing semiconductor.

A comparison between the current density versus potential (*J*-*E*) behavior of a planar, single-crystalline Czochralski-grown p-Si (0.7 ohm cm) sample and a p-Si wire array is shown in Fig. 3. Under 60 mW cm^{-2} of 808 nm illumination (selected to produce a similar photon flux above the Si band gap as that obtained from broadband, 100 mW cm^{-2}, air mass 1.5 solar illumination), the planar electrodes typically yielded open-circuit voltages (V_{oc}) of 0.555 ±

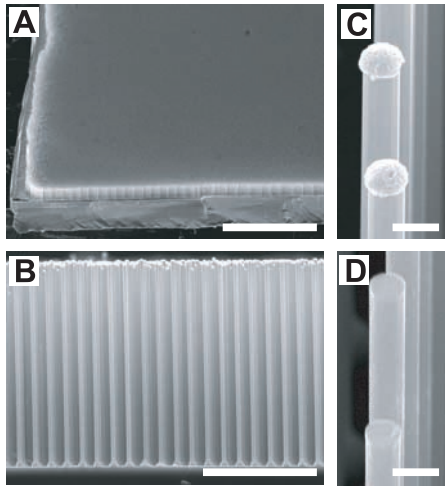

Fig. 1. (**A**) Scanning electron microscope image showing the p-Si wire arrays on a ~2-cm^2 wafer (scale bar, 600 μm). (**B**) Side view of a cleaved sample (scale bar, 50 μm). (**C**) Close-up showing the faceted wire and the copper catalyst tip before etching (scale bar, 2 μm). (**D**) Close-up showing the wire tops after etching with $FeCl_3$, KOH, and HF (scale bar, 2 μm).

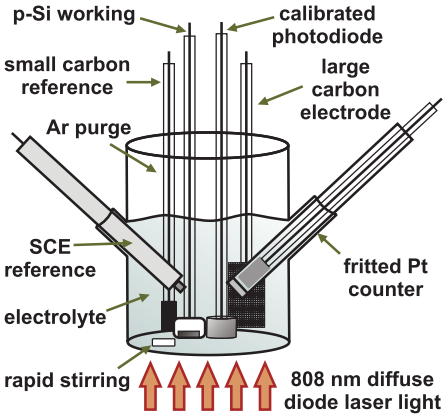

Fig. 2. Photoelectrochemical characterization was conducted in a glass cell configured so that the redox potential of the solution could be controlled versus a standard calomel reference electrode (SCE) and the incident light intensity could be measured in situ. The cell was filled with ~50 mL of aqueous electrolyte containing 0.5 M K_2SO_4 and 0.05 M methyl viologen dichloride (MV^{2+}) and buffered at pH = 2.9. The solution potential was driven to –0.60 V versus SCE by using the large carbon-cloth electrode as a working electrode and the frit-separated Pt mesh as a counter electrode, which turned the electrolyte deep purple-blue because of the formation of MV^+ radical (~ 3 mM). During photoelectrochemical characterization, the p-Si sample was used as the working electrode, the large carbon cloth as the counter electrode, and the small carbon cloth as the reference electrode.

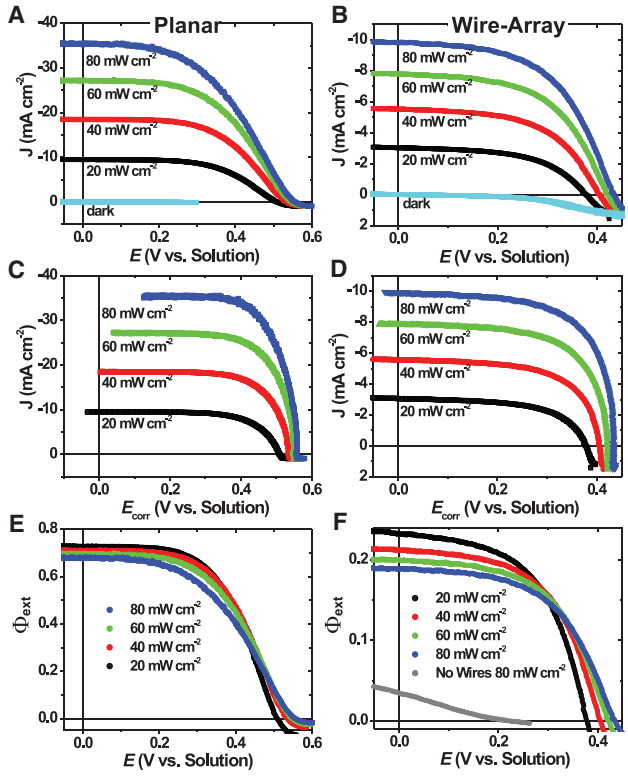

Fig. 3. Current-potential data as a function of 808-nm illumination intensity for (**A**) planar and (**B**) wire-array photoelectrodes. Solution absorbance is accounted for via the in situ measurement of the incident light intensity. In panels (**C**) and (**D**), the same data are displayed corrected for the solution effects, including uncompensated cell resistance (~20 ohms) and concentration overpotentials, so as to attain photoelectrode performance parameters inherent to the Si electrodes. The external quantum yield plotted in panels (**E**) and (**F**) was calculated on the basis of the incident light intensity, the sample area, and the measured photocurrent from panels (A) and (B), respectively. The performance of a wire-array sample in which the wires had been physically removed from the substrate confirmed that the p^+-Si substrate did not substantially contribute to the observed photoresponse.

0.015 V, short-circuit photocurrent densities (J_{sc}) of 27.9 ± 0.8 mA cm^{-2}, external quantum yields at short-circuit ($\Phi_{ext,sc}$) of 0.71 ± 0.02, fill factors (*ff*) of 0.51 ± 0.05, and photoelectrode energy-conversion efficiencies (η_{808}) of 12.9 ± 1.0% (across six devices; the uncertainty is reported as 1 SD). Correction for the concentration overpotential and uncompensated resistance losses (*15*, *19*) in the aqueous $MV^{2+/+}$ test electrolyte yielded the inherent photoelectrode properties under these conditions of ff_{corr} = 0.68 ± 0.05 and $\eta_{808,corr}$ = 17.4 ± 1.0%. Under the same conditions, wire-array samples exhibited V_{oc} = 0.41 ± 0.04 V, J_{sc} = 7.7 ± 0.9 mA cm^{-2}, $\Phi_{ext,sc}$ = 0.20 ± 0.02, *ff* = 0.50 ± 0.10, and η_{808} = 2.6 ± 0.4% (across six devices). For the specific wire-array electrode displayed in Fig. 3, V_{oc} = 0.42 V, J_{sc} = 7.9 mA cm^{-2}, $\Phi_{ext,sc}$ = 0.20, *ff* = 0.55, and η_{808} = 3.0%. The inherent photoelectrode properties of this electrode were ff_{corr} = 0.65 and $\eta_{808,corr}$ = 3.6%.

The V_{oc} of a semiconductor junction is given by

$$V_{oc} = (nk_BT/q)\ ln\ (J_{ph}/\gamma J_o) \quad (1)$$

where n is the diode quality factor, k_B is the Boltzmann constant, T is the temperature (in Kelvin), q is the (unsigned) charge on an electron, J_{ph} is the photocurrent density, J_o is the exchange current density, and γ is the ratio of the actual junction area to the projected surface area of the electrode, that is, the roughness factor (*2*, *6*). The planar p-Si samples exhibited a V_{oc} that was near the bulk recombination limit of 0.60 V (at $J_{ph} = J_{sc}$ = 27 mA cm^{-2}), which was calculated from the value of J_o produced by the known bulk properties and effective minority-carrier diffusion length of the p-Si sample investigated (*20*), attesting to the high quality of the semiconductor/liquid junction obtained in this test electrolyte system.

Equation 1 implies that for each 10-fold increase in γ, the reduced splitting in the quasi-Fermi levels when the photogenerated charge carriers are diluted over the larger junction area will decrease V_{oc} at room temperature by at least 59 mV. Because γ ~ 10 for the wire-array samples fabricated here, the V_{oc} is thus within ~50 mV of that expected on the basis of the behavior of the planar cells at similar J_{sc} levels. This result suggests that these p-Si microwires are largely free of electronically deleterious defects or impurities that would lower the V_{oc} substantially beyond that dictated by purely geometric considerations.

Optimized wire-array solar cells would exhibit a much higher J_{sc} than the values observed in the test samples. To evaluate the reasons for the lower J_{sc} values of the wire arrays relative to the planar Si sample, Φ_{ext} was measured for the electrodes as a function of angle (θ, where θ = 0° is normal incidence), using excitation with a laser spot (~1 mm^2) much smaller than the sample area (Fig. 4). At θ = 60°, at which the light path through the array was substantially increased relative to that for θ = 0°, Φ_{ext} approached 0.7. Accounting for reflection and residual absorption by the photo-inactive p^+ substrate, the internal quantum yield (Φ_{int}) was thus near unity. This conclusion is consistent with the observation that Φ_{ext} = ~0.2 at normal incidence for the wire array even though the specific growth template produced wires that filled only 4% of the optical plane.

Under 100 mW cm^{-2} of simulated solar illumination in the same electrolyte that did not contain MV^+ (so as to eliminate visible light absorption), these p-Si wire arrays exhibited J_{sc} values of ~9 to 11 mA cm^{-2} (*21*). The theoretical J_{sc} limit for Si under such conditions is 43 mA cm^{-2}, and in practice optical reflection losses reduce this value to ~35 mA cm^{-2}. Hence, the J_{sc} observed for the wire-array sample is larger, by a factor of ~6, than the J_{sc} expected for complete light absorption and unity internal quantum yield by an array that captured only 4% of the incident photons (based on the geometric filling fraction of the optical plane). This observation indicates substantial internal light scattering and optical focusing into the Si regions of the wire arrays.

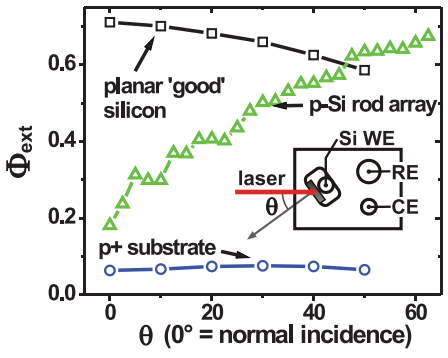

Fig. 4. Angle-resolved photocurrent measurements performed with a 633-nm He-Ne laser (power = 2.6 μW). Measurements were conducted in the absence of the MV^+ radical cation in order to avoid issues associated with oxygen sensitivity and solution absorbance (*29*). The uncertainties associated with the measurement of Φ_{ext} and θ were ±0.003 and ±0.5°, respectively. (Inset) Schematic of the cell, showing the rotating p-Si working electrode (WE) that was biased during measurement at −0.45 V versus SCE, the reference electrode (RE), and the counter electrode (CE).

Because in this work the internal quantum yields have been determined to approach unity, methods for achieving nearly complete light absorption [by increasing the wire-array packing fraction from the current value of ~4% or by improving optical trapping effects (*21*), for instance by placing dielectric scattering elements in between the wires] would thus be expected to produce a fourfold increase in the short-circuit photocurrent density to values comparable with or in excess of those observed for Si single crystals under the same conditions.

As shown in Fig. 3, the fill factor was similar for both the planar samples and the p-Si wire arrays. The *J-E* behavior of the planar sample indicates that with sufficient mass transport, either by active convection (as used here) or by passive means through the use of a thin-layer cell configuration (*22*), this specific test electrolyte allows for $J_{sc} > 35$ mA cm^{-2} with low accompanying mass-transport–based overpotentials. Consistent with these observations, we found that increasing the concentration of MV^{2+} to 0.1 M had little effect on the *J-E* behavior. However, in order to use wire arrays that produce increased photocurrent densities due to optimal light absorption at normal incidence, mass-transport limitations of redox species in the internal volume of the wire-array structure and unwanted optical absorption due to the ineffective removal of the colored MV^+ species within this volume must be minimized. Similar challenges have been overcome in the optimization of dye-sensitized nanocrystalline TiO_2 solar cells (*23*).

Provided that the optical absorption of the redox species can be minimized, improvements in J_{sc} to 35 mA cm^{-2}, while retaining the open-circuit voltages and uncorrected fill factors displayed in Fig. 3B, would imply that photoelectrode efficiencies >8% are attainable under air mass 1.5 conditions (*24*). The importance of the observations reported here, however, is not whether optimized photoelectrochemical solar cells can be prepared by using this specific test electrolyte but rather that the inherent performance of these p-Si wire arrays in a radial junction geometry allows, conceptually, the development of efficient photovoltaic and/or photoelectrochemical energy-conversion devices based on a wire-array platform, provided that the device-related engineering issues are satisfactorily addressed.

The use of Cu as the VLS-growth catalyst (*25*), as opposed to Au (*3*, *4*, *8*, *10*), probably contributes to the relatively high inherent energy-conversion performance of these p-Si wire-array devices. Cu concentrations of less than 10^{18} cm^{-3} appear to have little effect on the performance of planar Si solar cells (*26*). Apparently, the high diffusivity (2.8×10^{-7} cm^2 s^{-1} at 300 K) and the large energy barrier for precipitate nucleation of Cu in p-Si allow for collection of Cu at surfaces and defects, thus leaving the bulk Si largely free of Cu (*27*). At the growth temperature (1000°C), the wires are presumably saturated (~5×10^{17} cm^{-3}) with Cu, but upon cooling Cu probably segregates to the wire surface, allowing for its subsequent removal via chemical etching before testing of the resulting devices. No Cu was detected on the etched wire samples by using surface-sensitive techniques such as x-ray photoelectron spectroscopy, although more detailed experiments are needed to quantify the location and removal of Cu impurities that might originate from the VLS catalyst (*28*).

Although Si wire arrays and dye-sensitized nanocrystalline TiO_2 photoelectrodes both have absorbers with high aspect ratios, the properties of these two systems are governed by different physical principles. Dye-sensitized nanocrystalline TiO_2 photoelectrochemical cells do not have an appreciable space-charge layer in the TiO_2, and charge-carrier separation after dye-based light absorption relies on diffusion, along with the asymmetric, slow interfacial charge-transfer kinetics of the I_3^-/I^- redox couple that is uniquely effective in preventing electron-hole recombination in such systems. In contrast, charge-separation in the Si wire-array system is driven by an interfacial electric field in the space-charge region of the radial junction, and charge-carrier transport and recombination are governed by conventional device-physics principles implemented in a radial geometry (*2*). Thus, in addition to lacking a surface-bound dye for light absorption, Si wire arrays should be useful both as photoanodes and photocathodes in contact with a variety of aqueous and nonaqueous electrolytes that contain well-developed, kinetically facile, one-electron redox couples, as well as for photoelectrochemical H_2 evolution from water, given the integration of appropriate electrocatalysts (*1*).

References and Notes

1. R. N. Dominey, N. S. Lewis, J. A. Bruce, D. C. Bookbinder, M. S. Wrighton, *J. Am. Chem. Soc.* **104**, 467 (1982).
2. B. M. Kayes, H. A. Atwater, N. S. Lewis, *J. Appl. Phys.* **97**, 114302 (2005).
3. A. P. Goodey, S. M. Eichfeld, K. K. Lew, J. M. Redwing, T. E. Mallouk, *J. Am. Chem. Soc.* **129**, 12344 (2007).
4. J. R. Maiolo 3rd *et al.*, *J. Am. Chem. Soc.* **129**, 12346 (2007).
5. E. C. Garnett, P. D. Yang, *J. Am. Chem. Soc.* **130**, 9224 (2008).
6. J. M. Spurgeon, H. A. Atwater, N. S. Lewis, *J. Phys. Chem. C* **112**, 6186 (2008).
7. B. Z. Tian *et al.*, *Nature* **449**, 885 (2007).
8. B. Tian, T. J. Kempa, C. M. Lieber, *Chem. Soc. Rev.* **38**, 16 (2009).
9. M. D. Kelzenberg *et al.*, *Nano Lett.* **8**, 710 (2008).
10. L. Tsakalakos *et al.*, *Appl. Phys. Lett.* **91**, 3 (2007).
11. T. Stelzner *et al.*, *Nanotechnology* **19**, 295203 (2008).
12. K. Peng *et al.*, *Small* **1**, 1062 (2005).
13. C. Colombo, M. Heiss, M. Gratzel, A. F. I. Morral, *Appl. Phys. Lett.* **94**, 3 (2009).
14. R. S. Wagner, W. C. Ellis, *Appl. Phys. Lett.* **4**, 89 (1964).
15. Materials and methods are available as supporting material on *Science* Online.
16. B. M. Kayes *et al.*, *Appl. Phys. Lett.* **91**, 103110 (2007).
17. D. C. Bookbinder, N. S. Lewis, M. G. Bradley, A. B. Bocarsly, M. S. Wrighton, *J. Am. Chem. Soc.* **101**, 7721 (1979).
18. J. F. Stargardt, F. M. Hawkridge, *Anal. Chim. Acta* **146**, 1 (1983).
19. T. W. Hamann, F. Gstrein, B. S. Brunschwig, N. S. Lewis, *J. Am. Chem. Soc.* **127**, 7815 (2005).
20. N. S. Lewis, *J. Electrochem. Soc.* **131**, 2496 (1984).
21. O. L. Muskens, J. G. m. Rivas, R. E. Algra, E. P. A. M. Bakkers, A. Lagendijk, *Nano Lett.* **8**, 2638 (2008).
22. J. F. Gibbons, G. W. Cogan, C. M. Gronet, N. S. Lewis, *Appl. Phys. Lett.* **45**, 1095 (1984).
23. M. Grätzel, *Nature* **414**, 338 (2001).
24. The efficiency is calculated as $J_{sc} * V_{oc} * ff$/(100 mW cm^{-2}), where J_{sc} is assumed to be 35 mA cm^{-2}, $V_{oc} = 0.42$, and $ff = 0.55$. These photoelectrode parameters are consistent with those estimated from air mass 1.5 illumination.
25. V. Schmidt, J. V. Wittemann, S. Senz, U. Gosele, *Adv. Mater.* **21**, 2681 (2009).
26. J. R. Davis *et al.*, *IEEE Trans. Electron. Dev.* **27**, 677 (1980).
27. A. A. Istratov, E. R. Weber, *J. Electrochem. Soc.* **149**, G21 (2002).
28. M. C. Putnam *et al.*, *Nano Lett.* **8**, 3109 (2008).
29. These current densities were measured in the absence of MV^+ radical cation. This configuration allows for testing in an optically transparent solution and hence measurement of accurate values for J_{sc} under solar simulation. Under these conditions, the cell does not operate as a regenerative photovoltaic because the potentiostat drives oxygen evolution at the Pt counter (as opposed to MV^+ oxidation).

30. We acknowledge the Stanford Global Climate and Energy Project and the U.S. Department of Energy (grant DE-FG02-05ER15754) for financial support. S.W.B. thanks the Kavli Nanoscience Institute for a postdoctoral fellowship. L. O'Leary is thanked for her contributions. The authors have filed U.S. patent applications (20090020150 and 20090020853) related to this work.

Supporting Online Material

www.sciencemag.org/cgi/content/full/327/5962/185/DC1
Materials and Methods
References

19 August 2009; accepted 10 November 2009
10.1126/science.1180783